ORIGINAL SCIENTIFIC PAPER

CROATICA CHEMICA ACTA

Croat. Chem. Acta **2020**, *93*(1), 15–22
Published online: April 24, 2020
DOI: 10.5562/cca3606

HKD 1926

Structural Characterization of β-Glycolaldehyde Dimer

Vlasta Mohaček-Grošev,[1,*] Biserka Prugovečki,[2] Stjepan Prugovečki[3]

[1] Center of Excellence for Advanced Materials and Sensing Devices, Ruđer Bošković Institute, Bijenička c. 54, 10000 Zagreb, Croatia
[2] Department of Chemistry, Faculty of Science, University of Zagreb, Horvatovac 102a, 10000 Zagreb, Croatia
[3] Malvern Panalytical B.V., Lelyweg 1, 7602 EA Almelo, The Netherlands
* Corresponding author's e-mail address: mohacek@irb.hr

RECEIVED: December 23, 2019 * REVISED: April 15, 2020 * ACCEPTED: April 21, 2020

Abstract: Structural characterization of the β-polymorph of glycolaldehyde dimer by powder X-ray diffraction, Raman and infrared spectroscopies is described. The previously described α-polymorph and the β-polymorph both crystallize in the monoclinic crystal system, space group $P2_1/c$, but with different cell parameters. There are no significant differences in the glycolaldehyde dimer molecular structure, the molecules in both polymorphs are *trans*-isomers with the hydroxyl groups in axial positions. The two polymorphs have a different arrangement of the glycolaldehyde dimer molecules. In the previously reported α-polymorph the molecules are arranged in hydrogen bonded layers parallel to (100) while in the β-polymorph the hydrogen bonded molecules are arranged in a three-dimensional network. Theoretically calculated Gibbs free energy as well as differential scanning calorimetry indicate β-polymorph to be the stable crystal phase of glycolaldehyde.

Keywords: glycolaldehyde dimer, crystal structure, Raman, infrared, X-ray powder diffraction, biodegradable polymer.

INTRODUCTION

THE emerging new technologies of additive manufacturing together with expanding requirements for degradable materials have stimulated research and development of new biopolymers. Besides poly(lactic acid), PLA, and poly(glycolic acid), PGA, poly(dioxanone) has also been approved by Food and Drug Administration Agency as a suture material.[1] The degree of crystallinity and the melting point of PLA are determined by the nature of lactide dimers which are used to produce it – such as L,L-lactide, D,D-lactide or racemic D,L-lactide.[2] Whereas poly(dioxanone) can be the result of ring opening polymerization, a recently patented poly(2,5-dihydroxy-1,4-dioxane), PDHDO, uses glycolaldehyde dimer molecules as monomers linked together via glycosidic linkages.[3]

Glycolaldehyde, CHOCHOH, is at room temperature a polycrystalline solid, existing in the form of 2,5-dihydroxy-1,4-dioxane or glycolaldehyde dimer, whose α- and β-polymorphs were first distinguished by Kobayashi et al.[4] The conformation of hydroxyl groups was assumed equatorial in the α-phase and axial in the β-phase. Recently, the crystal structure of the α-polymorph was solved by Mohaček-Grošev et al.[5] and it was found that molecules crystallize with axially placed OH groups. On cooling, α-phase transforms into the third γ-phase below 80 K.[6]

Dissolving of glycolaldehyde is a complex, time dependent process. NMR spectroscopy proved to be a very fruitful method for obtaining information on glycolaldehyde solutions in deuterated dimethylsulfoxide (DMSO-d_6)[7–9] or in water[9–11]. It turns out that dimer ring exists in more than two interchanging configurations, monomers and open chain dimers emerge, as well as new compounds such as 2-methoxy-4-hydroxy-1,3-dioxolane[7–11]. In all cited works, by inspecting time dependence of ^{1}H NMR spectra, the number of attributed molecular species ranged from at least three in DMSO-d_6[9] to nine in water.[11] Therefore, the observation of Luebben et al.,[12] although given tentatively, that a single conformer of glycolaldehyde is present in the DMSO-d_6 solution seems at odds with previous NMR studies.

Recently Raman study accompanied with extensive ab initio calculations of time dependence of alkaline and water glycolaldehyde solutions was performed, whereby

authors gave the ratio of hydrated aldehyde to aldehyde monomer to dimer forms in water solution as 4 : 0.25 : 1.[13] They confirmed that enediol form of glycolaldehyde exists only in alkaline solutions and furthermore established that only the Z form of enediolate participates in exchange with the aldo form. Another study of monomer and oligomer equilibria used NMR spectra to determine concentrations of different species in glycolaldehyde water solutions and calculated reaction free energies and barriers for interconversion of different species.[10]

Here we report the crystal structure of β-glycolaldehyde whose Raman and infrared spectra are completely in accord with the data of the β-polymorph provided by Kobayashi et al.[4] Observed vibrational bands for α- and β-polymorph are discussed and compared with the bands of 1,4-dioxane. A complete periodic density functional theory calculation of phonon modes was performed for both polymorphs, and their Gibbs free energies obtained. Together with the results of differential scanning calorimetry measurements these new theoretical and experimental data can help in determination of the stable crystal structure of the glycolaldehyde dimer.

EXPERIMENTAL

Glycolaldehyde dimer, purity > 98 %, was purchased from Fluka and used without further purification.

Far infrared spectra of powdered sample applied on polyethylene window were recorded in transmission mode by Perkin-Elmer GX spectrometer, equipped with DTGS detector, in absorption mode with 2000 scans and 1 cm^{-1} resolution. Spectral range was from 140 to 700 cm^{-1}. Infrared spectrum of β-glycolaldehyde dimer in the mid IR range was obtained by pressing the powder in KBr pellet and recording in transmission mode by the same FTIR spectrometer, this time in the range 370–4000 cm^{-1}.

Raman spectra were recorded at room temperature with HORIBA JobinYvon T64000 triple monochromator in the triple subtractive mode using microscope with objective 50× LWD, equipped with CCD detector. Low temperature Raman spectra were recorded with DILOR Z24 triple monochromator in sequential mode with step 0.5 or 1 cm^{-1}. Sealed glass capillary with powder was mounted on the cold finger of the CTI Cryogenics model 22 cryostat with helium closed cycle with Lake Shore Cryotronics temperature controller. The accuracy of spectral bands positions was better than one cm^{-1}.

Differential scanning calorimetry experiments were performed with a Netzsch DSC 200 instrument having a liquid nitrogen cooling system in the helium atmosphere. Heating and cooling rates were 2.0, 5.0 and 15.0 K min^{-1} for the α- polymorph, and 5 K min^{-1} for the β-polymorph.

X-ray Powder Diffraction

Crystal structure of β-glycolaldehyde dimer was solved from laboratory X-ray powder diffraction data. The powder X-ray data were collected on a Malvern Panalytical Empyrean diffractometer configured for the focusing capillary transmission geometry with PIXcel^{3D} detector, using Cu$K_{\alpha 1}$ radiation. The sample was contained in a 0.5 mm radius borosilicate glass capillary which was rotating during the measurement. The diffracted intensities were collected at room temperature in the range from16.5° to 120.0° (2ϑ). The data collection parameters are given in Table 1. Powder pattern was indexed by DICVOL 04 [14] and also confirmed by TREOR,[15] both embedded in the Malvern Panalytical HighScore Software Suite.[16] The unit cell parameters used

Table 1. Crystal data and structure refinement parameters for β-glycolaldehyde dimer.

Crystal data	
Formula	$C_4H_8O_4$
M_r	120.10
Powder colour	yellow
Crystal System	monoclinic
Space group	*P* 21/*c*
Unit cell parameters	
a, *b*, *c* / Å	9.80132(1), 6.13522(1), 9.76368(1)
α, *β*, *γ* / °	90, 119.812(1), 90
V / Å^3	509.422(5)
Z	4
D_{calc} (g cm^{-3})	1.566
Temperature / K	293
Wavelength / Å	1.540598
Data collection	
Diffractometer	Malvern Panalytical Empyrean
Specimen mounting	Glass capillary
Data collection mode	Transmission
2Θ values (°)	$2\Theta_{min}$ = 16.5, $2\Theta_{max}$ = 120.0, $2\Theta_{step}$ = 0.0066
Refinement	
R_p, R_{wp}	0.0319, 0.0477
Goodness-of-fit	1.703
2Θ values (°)	$2\Theta_{min}$ = 16.5, $2\Theta_{max}$ = 100.0
No. of independent non-hydrogen atoms	8
No. of refined parameters	32 (structure)
H-atom treatment	H-atom parameters constrained

for structure solving were refined and the space group confirmed by Pawley fitting in the HighScore Software Suite. Intensities extracted by Pawley fit were used for structure solving. The structure was solved by direct methods using SIR92 software.[17] The structural model obtained from direct methods was used in the final Rietveld refinement. The Rietveld refinement in 2ϑ range from 16.5° to 100.0° was carried out using Malvern Panalytical HighScore Software Suite. The background was refined using the type 1 Chebichev polynomial function. The Finger, Cox, Jephcoat diffraction peak asymmetry correction was applied.[18] Unit cell parameters, scale factors, atomic coordinates and isotropic atomic displacement parameters and profile parameters of Pseudo-Voigt profile function were refined in the final Rietveld fit (Figure S1, Supporting Information). No restrains or constraints on atomic coordinates and isotropic displacement parameters were used in the final Rietveld fit. Before the final refinement, the hydrogen atoms were introduced from geometrical arguments (C–H = 0.97 Å for -CH2-groups, C–H = 0.98 Å for tertiary CH groups and O–H = 0.82 Å for hydroxyl groups, Uiso (H) = 0.075) by SHELXL-97 program.[19]

Computation of Vibrational Transitions

For *ab initio* calculation of phonons, the CRYSTAL09 program was used,[20] running on HP Z640 workstation using 8 processors. Atomic positions in the unit cell of the β-polymorph were optimised starting from crystal geometry obtained by powder X-ray diffraction which provided sufficient precision for the calculation to converge and later give all positive vibrations. Three lowest modes of the total of 192 modes were acoustic modes with zero frequencies. For oxygen, carbon and hydrogen atoms basis set of Gatti was taken.[21] Density functional theory as implemented by the correlation functional of Lee, Yang, and Parr with generalized gradient approximation,[22] and the exchange functional of Becke[23] (known as B3LYP) was used. The 35 % of mixing of old wavefunction with the new one was applied in each cycle. The convergence criterion for energy was 10^{-10} Ha. The output is available as a Supplementary information.

Normal modes of 1,4-dioxane were obtained from an *ab initio* calculation of force constant matrix using Gaussian03 program suite,[26] followed by calculation of potential energy distribution with MOLVIB[27] and BALGA[28,29] programs.

RESULTS AND DISCUSSION

To prove that the β-glycolaldehyde phase is identical with the β-phase of Kobayashi et al.,[4] one can compare the Raman and infrared spectra obtained and displayed in Figures 1 and 2 with spectra from ref. [4]. An excellent agreement is found.

X-ray Crystallography

β-Glycolaldehyde crystallizes as a dimer with the 1,4-dioxane ring in the chair conformation and OH groups in axial positions (Figure 3). The asymmetric unit contains two halves of the symmetrically independent glycolaldehyde dimer molecules which lie on inversion centers. Analysis of the bond lengths revealed that the C–O bonds in one symmetrically independent glycolaldehyde dimer molecule in the β-form is lengthened in comparison to the previously reported α-glycolaldehide dimer[5] (Supporting Information, Table S1).

A common feature of both polymorphic forms (α and β) is the association of the molecules by O–H···O hydrogen bonds. In the previously reported structure of α-glycolaldehyde both oxygen atoms (hydroxyl and 1,4-dioxane) are involved in hydrogen bonding while in the structure of β-glycolaldehyde only the oxygen atoms from the hydroxyl groups are hydrogen bond donors and acceptors. In the

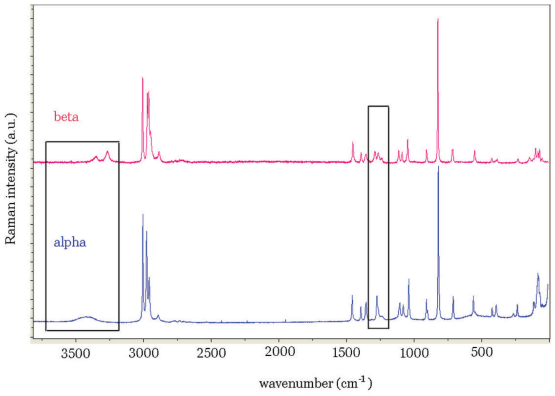

Figure 1. Comparison of Raman spectra of α- and β-glycolaldehyde. Rectangular frames point out spectral differences.

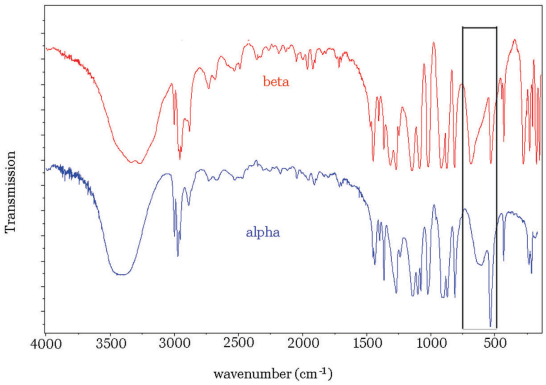

Figure 2. Comparison of infrared spectra of α- and β-glycolaldehyde. Rectangular frame points out spectral differences of the OH torsion bands.

crystal structure of β-glycolaldehyde two symmetrycally independent glycolaldehyde dimer molecules are connected by hydrogen bonds O2–H2···O4 [*x, y,* 1 + *z*] and O4–H4···O2 [*x*, ½ - *y*, -1/2 + *z*] (Figure 4). In the reported β-glycolaldehyde dimer, the molecules are arranged in a hydrogen bonded 3D network while in the previously reported α-glycolaldehyde layers parallel to (100) are formed. The final Rietveld plot of β-glycolaldehyde dimer is presented in Figure 5.

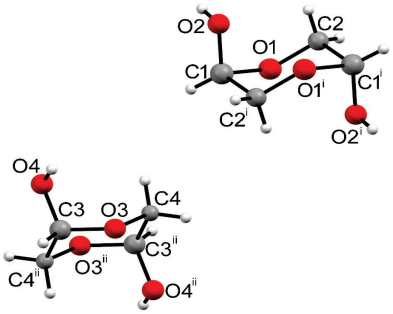

Figure 3. The molecular structures of two symmetrycally independent β-glycolaldehyde molecules (symmetry code: [i] –*x*, –*y*, 1–*z*; [ii] –*x*, 1–*y*, 1-*z*).

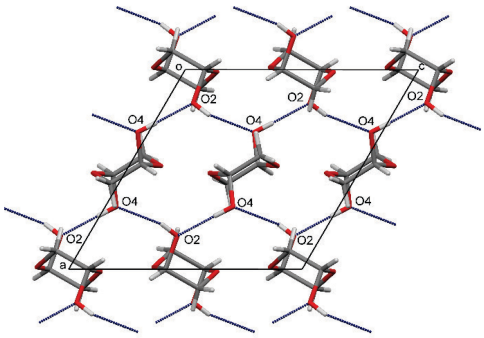

Figure 4. The crystal packing diagram of β-glycolaldehyde viewed along the *b*-axis.

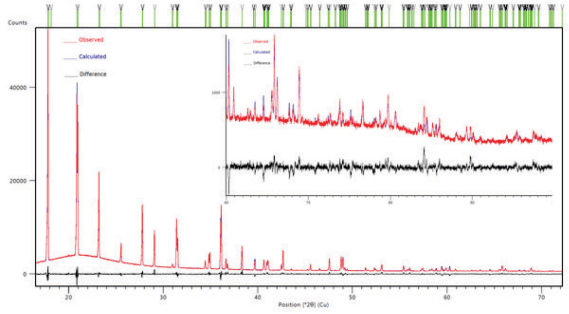

Figure 5. The final Rietveld plot of β-glycolaldehyde dimer in 2ϑ range from 16.5° to 100.0°, (R_p = 0.0319, R_{wp} = 0.0477). Red-observed pattern, blue-calculated, black-difference. Green vertical bars indicate Bragg reflections.

Vibrational Analysis

Here, new information in the form of low frequency Raman spectra from 9 cm^{-1} and previously undetected Raman bands above 3000 cm^{-1} are presented (see Supplementary Table S2 for complete list of observed bands).

Glycolaldehyde dimer is a centrosymmetric molecule which differs from 1,4-dioxane (we refer to it as dioxane from now on) in two axially placed hydroxyl groups, hence many vibrational bands observed for polycrystalline glycolaldehyde occur in close proximity of dioxane bands (see Supplementary tables S3 and S4). Normal mode analysis for glycolaldehyde dimer with axially placed hydroxyl groups was presented in previous publication,[5] therefore we briefly point out main spectral differences between pol ymorphs α and β and polycrystalline dioxane. In Table 2 the majority of phonon modes of β-polymorph which involve hydroxyl groups are listed.

Dioxane molecule has $\mathbf{C_{2h}}$ point group symmetry. As a consequence, among 36 normal modes, 10 A_g and 8 B_g modes are Raman active and 9A_u and 9 B_u modes are infrared active in the vibrational spectrum of liquid (Supplementary tables S3 and S4). In the crystal, molecules occupy sites with $\mathbf{C_i}$ symmetry and are arranged in the monoclinic $P2_1/n$

Table 2. Comparison of selected observed Raman and infrared vibrational modes of the β- glycolaldehyde with the values calculated using CRYSTAL09 program.

Raman observed 295 K phase β	Infrared observed 295 K phase β	Calculated values and symmetry	Approximate description
3351 w	3460 s,sh	3527 B_u	
		3547 A_g, 3520 B_g	
3265 w	3339 s,vbr	3504 A_u	OH stretching
	3267 s,vbr	3471 A_u	
		3488 B_g. 3428 A_g	
	3167 ms,sh	3428 B_u	
	1364 ms	1361 B_u	
	1316 s,br	1337 A_u	
1288 mw		1384 A_g	C-O-H bending
		1345 B_g, 1335 B_g, 1327 A_g	
	1270 s	1326 A_u, 1307 B_u, 1299 A_u, 1298 B_u	
1264 mw		1296 A_g, 1296 B_g, 1291 B_g	
	1249 m	1292 A_u 1290 B_u	
1240 w		1280 A_g	
	687 s	772 B_u, 769 A_u	C-C-O-H torsion
		748 B_g, 743 A_g	
		711 B_g, 706 A_g	

space group with two molecules per unit cell.[31] Here one expects 21 $A_g \oplus$ 21 $B_g \oplus$ 21 $A_u \oplus$ 21 B_u phonons, of which below 250 cm^{-1} using rigid molecule approximation one predicts six Raman active and three infrared active bands:

$$\Gamma_{ext} = 3\ A_g \oplus 3\ B_g \oplus 2\ A_u \oplus\ B_u.$$

Above 250 cm^{-1} the number of dioxane internal modes predicted is

$$\Gamma_{int} = 18\ A_g \oplus 18\ B_g \oplus 18\ A_u \oplus 18\ B_u.$$

There are four molecules in the unit cell of β-glycolaldehyde (twice as many as in the α-polymorph), therefore the number of expected phonons below 250 cm^{-1} is twelve in Raman and nine in the infrared spectrum

$$\Gamma_{ext}^{\beta} = 6\ A_g \oplus 6\ B_g \oplus 5\ A_u \oplus\ 4\ B_u,$$

and the number of internal modes is

$$\Gamma_{int}^{\beta} = 42\ A_g \oplus 42\ B_g \oplus 42\ A_u \oplus 42\ B_u.$$

There are eleven phonon bands observed in Raman spectrum of β-polymorph below 250 cm^{-1} at 295 K (Supplementary table S2). A comparison of the observed and calculated Raman phonon bands is shown in Figure 6. Low

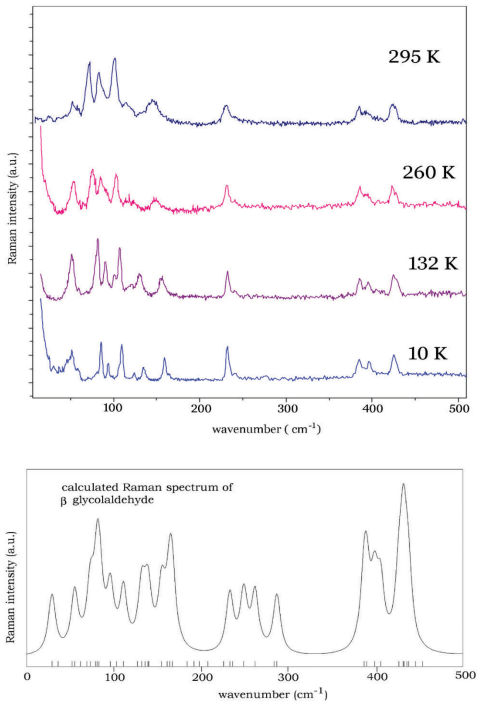

Figure 6. Observed and calculated low frequency Raman spectra of the β-glycolaldehyde.

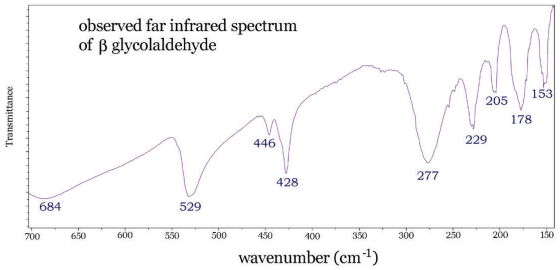

Figure 7. Observed far-infrared spectrum of the β-glycolaldehyde in the 140 – 700 cm^{-1} interval.

frequency bands observed in Raman spectrum consist generally of molecular librations, while in far infrared spectrum (Figure 7) these modes have translatory nature. In systems having hydrogen bonded molecules, one can observe additionally stretching of the hydrogen bond O-H···O, like in oxalic acid dihydrate at 280 cm^{-1},[25] and it is necessary to study O-D···O in the deuterated molecular crystal as well in order to properly identify this mode.

Among internal vibrational modes, those with lowest wavenumbers are ring torsion and ring bending modes. Whereas the lowest internal modes of dioxane liquid are observed at 274 (B_u) and 288 cm^{-1} (A_u) in the infrared spectrum,[30] in β-glycolaldehyde the lowest internal mode predicted by rigid molecule approximation would be assigned as B_u mode calculated at 161 cm^{-1} by the CRYSTAL09 program. Inspection of this mode using MOLDRAW program[24] reveals it as both ring bending and hydrogen bond bending mode that can be assigned to the 153 cm^{-1} band observed in the far infrared spectrum (Figure 7). Hydrogen bond bending is also present in the motion of atoms displayed in the A_u mode calculated to be at at 184 cm^{-1} and possibly assigned to 178 cm^{-1} infrared band (Figure 7). Bending of C-O-C ring angles is characteristic for the B_u phonon calculated at 208 cm^{-1} and assigned to the infrared band at 205 cm^{-1}, and the Raman active A_g mode calculated at 233 cm^{-1} and assigned to the band at 232 cm^{-1} (Figure 6, Table S2).

Comparing the observed Raman bands of the β-glycolaldehyde phase with the calculated vibrations of the free dimer,[5] the bands at 385, 392 and 424 cm^{-1} are assigned to dioxane ring deformation modes, and the bands at 544, 556, and 560 cm^{-1} to O-C-O(H) bending vibrations. The torsion of OH groups, while barely visible in the Raman spectrum (486 cm^{-1} band is very weak and broad), is on the other hand assigned to strong and broad bands at 610 and 687 cm^{-1} in the infrared spectrum (Table 2). Vibrational modes of the CH_2 groups do not differ significantly from their positions in the α crystal phase (Figures 1 and 2), and the Raman band at 1105 cm^{-1} is assigned to CH_2 rocking motion. The 1455 cm^{-1} Raman and 1449 and 1471 infrared bands are interpreted as scissoring

motions. The C-H bending motion is coupled with C-O-H bending in the 1240–1370 cm^{-1} interval (Table 2 and Supplementary table S2). Strong C-O and C-C stretching modes are predicted in Raman spectrum at 810 cm^{-1} and 908 cm^{-1} in the infrared spectrum for free dimer with axial OH groups.[5] In the crystal, strong bands corresponding to these modes are observed at 822 cm^{-1} in Raman and at 874 and 902 cm^{-1} in the infrared spectrum of the crystal. The calculated values are somewhat higher, being 836, 839, 841 and 849 cm^{-1} for the Raman active vibrations. In the region of CH stretching vibrations the calculated CH stretching vibration is coupled with stretching vibrations of both CH_2 groups, and the calculated values for Raman active modes are 3086 cm^{-1} and 3085 cm^{-1}, which are higher than the observed values of 2967 cm^{-1} and 2958 cm^{-1} (Table S2).

Most prominent spectral differences between the two glycolaldehyde crystal phases concern COH groups, and are pointed out in rectangular boxes in Figs 1 and 2. The 600–750 cm^{-1} interval in the infrared spectrum comprises broad bands attributed to the torsion of OH groups, while it is in the 1240–1370 cm^{-1} interval that the bending motion of the hydroxyl groups dominates. In particular we stress the difference in the number of the observed different ν(OH) stretching modes in Raman spectrum: there are two bands observed at 3265 and 3353 cm^{-1} at 295 K in the β phase, and only one broad band in the Raman spectrum of the α phase at 3433 cm^{-1} (Fig 1). Temperature dependent Raman spectra of the second crystal phase shown in Figures 6 and 8, and Supplementary Figure S1, confirm the stability of the β phase with temperature. Two distinct OH stretching bands are in accord with the structural motif in the β crystal phase which disposes with two molecules having two different O-H···O contacts equal to 2.641 Å and 2.848 Å. On the contrary, all O-H···O distances in the α phase are of equal distance: 3.027 Å.

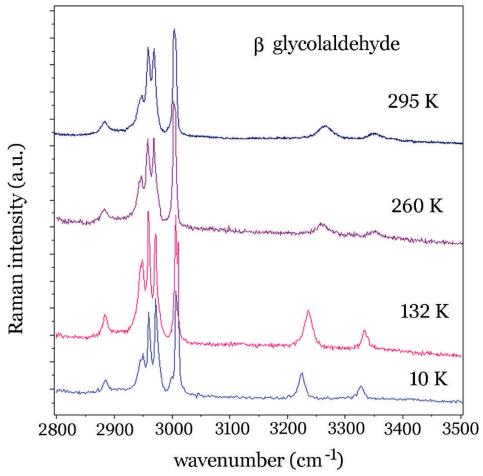

Figure 8. Observed Raman spectrum of β-glycolaldehyde in the 2800–3500 cm^{-1} interval at 295 K, 260 K, 132 K and 10 K.

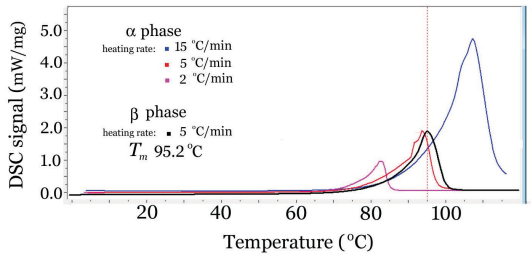

Figure 9. Differential scanning calorimetry measurements of glycolaldehyde with different heating rates of 2 K min^{-1}, 5 K $min^{-1}$and 15 K min^{-1} (α-polymorph) and 5 K min^{-1} (β-polymorph). Temperature T_{max} = 95.2 °C at which melting of β-polymorph occurs is denoted by vertical dashed line.

In order to gain more information on the relative stability of the two glycolaldehyde crystal structures, differential scanning calorimetry measurements were performed on the two samples (Figure 9). Two curves obtained with the heating rate of 5 K min^{-1} in the middle of the figure correspond to the α phase (T_{max} = 93.6 °C) and to the β phase (T_{max} = 95.2 °C). Heating curves of the α phase have a shoulder on the lower temperature side that probably corresponds to the γ phase.[6] Judging on the basis of the T_{max}, β-polymorph is more stable.

Theoretical prediction of the total Gibbs free energy per unit cell of the β-polymorph calculated by the CRYSTAL09 program gives the value at 295 K and 101325 Pa of - 49826.8728155 eV/cell, while for the α-polymorph it is –24913.2351268 eV/cell. Comparing these values as per one glycolaldehyde dimer molecule, one obtains -12456.6156 eV per each molecule for the α-polymorph, and –12456.7182 eV per each molecule for the β-polymorph. Therefore β-polymorph is predicted to be the more stable phase by 0.1 eV per molecule.

CONCLUSION

The crystal structure of the β-polymorph of glycolaldehyde dimer has been determined by the powder X-ray diffraction method. There are no significant differences in the molecular structures of the two polymorphs however the molecular packing is different. While in the α-glycolaldehyde dimer the molecules are interconnected by their hydroxyl groups and oxygen atoms from 1,4-dioxane rings into 2D layers, symmetrically independent molecules in the β-glycolaldehyde dimer are interconnected via their hydroxyl groups forming a 3D network. Raman and infrared spectra of the crystal have been assigned with the help of the CRYSTAL09 program, and by comparison with normal mode analysis for 1,4-dioxane and previous work on glycolaldehyde

dimer molecule.[5] Modes corresponding to hydrogen bonds – two different O-H···O contacts equal to 2.641 Å and 2.848 Å have been identified – have been listed. The crystal structure of the β-polymorph is the stable crystal structure based on the differential scanning calorimetry experiments and by the predictions of DFT calculations performed by the CRYSTAL09 program.

Acknowledgment. We acknowledge the help of prof. Hrvoje Ivanković from the Faculty of Chemical Engineering, University of Zagreb, in performing DSC measurements.
Funding: This work was partially supported by Centre of Excellence for Advanced Materials and Sensors, a project co-financed by the Croatian government and the European Union through the European regional development fund – The Competitivness and Cohesion Operational Programme (KK.01.1.1.01).

Supplementary Information. Supporting information to the paper is attached to the electronic version of the article at: https://doi.org/10.5562/cca3606.
CCDC 1966984 contains the supplementary crystallographic data for this paper. These data can be obtained free of charge via https://www.ccdc.cam.ac.uk/structures/, or by emailing data_request@ccdc.cam.ac.uk, or by contacting The Cambridge Crystallographic Data Centre, 12, Union Road, Cambridge CB2 1EZ, UK; fax: +44 1223 336033.
The output of the CRYSTAL09 program containing the calculated phonon frequencies is provided. Also, supplementary Figure S1 and supplementary Tables S1 to S7 are given.

PDF files with attached documents are best viewed with Adobe Acrobat Reader which is free and can be downloaded from Adobe's web site.

REFERENCES

[1] M. A. Sabino, J. L. Feijeo, A. J. Műller, *Macromol. Chem. Phys*. **2000**, *201*, 2687–2698.
[2] S. Inkinen, M. Hakkarainen, A.-C. Albertsson, A. Södergård, *BioMacromolecules* **2011**, *12*, 523–532. https://doi.org/10.1021/bm101302t
[3] S. DeVito Luebben, James William Raebiger, Aaron Jeremy Skaggs, can be found under https://www.google.com/patents/US9040635, accessed 23.12.2019.
[4] Y. Kobayashi, H. Takahara, H. Takahashi, K. Higasi, *J. Mol. Struct*. **1976**, *32*, 235–246. https://doi.org/10.1016/0022-2860(76)85002-8
[5] V. Mohaček-Grošev, B. Prugovečki, S. Prugovečki, N. Strukan, *J. Mol. Struct.* **2013**, *1047*, 209–215. https://doi.org/10.1016/j.molstruc.2013.05.006
[6] V. Mohaček-Grošev, *J. Raman Spectrosc.* **2005**, *36*, 453–461. https://doi.org/10.1002/jrs.1346
[7] Y. Kobayashi, H. Takahashi, *Spectrochimica Acta A* **1979**, *35A*, 307–314. https://doi.org/10.1016/0584-8539(79)80186-5
[8] C. I. Stassinopoulou, C. Zidrou, *Tetrahedron* **1972**, *28*, 1257–1263. https://doi.org/10.1016/S0040-4020(01)93550-1
[9] G. C. S. Collins, W. O. George, *J. Chem. Soc. B* **1971**, 1352–1355. https://doi.org/10.1039/j29710001352
[10] J. Kua, M. M. Galloway, K. D. Millage, J. E. Avila, D. O. De Haan, *J. Phys. Chem. A* **2013**, *117*, 2997–3008. https://doi.org/10.1021/jp312202j
[11] G. K. Glushonok, T. G. Glushonok, O. I. Shadyro, *Kinetics and Catalysis* **2000**, *41*, 620–624. https://doi.org/10.1007/BF02754560
[12] S. D. Luebben, J. W. Raebiger, in *Green Polymer Chemistry: Biobased Materials and Biocatalysis*; (Eds.: Smith et al.) ACS Symposium Series; American Chemical Society: Washington, DC, **2015**, pp. 305–328. https://doi.org/10.1021/bk-2015-1192.ch019
[13] L. M. Azofra, M. Mar Quesada-Moreno, I. Alkorta, J. R. Avilés-Moreno, J. Elguero, J. J. López-González, *Chem. Phys. Chem.* **2015**, *16*, 2226–2236. https://doi.org/10.1002/cphc.201500139
[14] A. Boultif and D. Louër, J. Appl. Cryst. **2004**, *37*, 724–731. https://doi.org/10.1107/S0021889804014876
[15] P.E. Werner, L. Erikson & M. Westdahl, *J. Appl. Cryst.* **1985**, *18*, 367–370. https://doi.org/10.1107/S0021889885010512
[16] T. Degen, M. Sadki, E. Bron, U. König, G. Nénert, *Powder Diffr*. **2014**, 29, S13–S18. https://doi.org/10.1017/S0885715614000840
[17] A. Altomare, G. Cascarano, C. Giacovazzo, M. C. Burla, G. Polidori, M. Camalli, *J. Appl. Cryst.* **1994**, *27*, 435–436. https://doi.org/10.1107/S002188989400021X
[18] L. W. Finger, D. E. Cox, A. P. Jephcoat, *J. Appl. Cryst.* **1994**, *27*, 892–900. https://doi.org/10.1107/S0021889894004218
[19] G. M. Sheldrick, *Acta Cryst.* **2008**, *A64*, 112–122. https://doi.org/10.1107/S0108767307043930
[20] R. Dovesi, R. Orlando, B. Civalleri, C. Roetti, V. R. Saunders, C. M. Zicovich-Wilson, *Z. Krist*. **2005**, *220*, 571–573. https://doi.org/10.1524/zkri.220.5.571.65065
[21] C. Gatti, V.R. Saunders, C. Roetti, *J. Chem. Phys.* **1994**, *101*, 10686–10696. https://doi.org/10.1063/1.467882
[22] C. Lee, W. Yang, R. G. Parr, *Phys. Rev. B* **1988**, *37*, 785–789. https://doi.org/10.1103/PhysRevB.37.785
[23] A. D. Becke, *Phys. Rev. A* **1988**, *38*, 3098–3100. https://doi.org/10.1103/PhysRevA.38.3098
[24] MOLDRAW, a program to display and manipulate molecular and crystalline structures, can be found under http://www.moldraw.unito.it/_sgg/m6_1.htm, accessed 13th April 2017.

[25] V. Mohaček-Grošev, J. Grdadolnik, J. Stare, D. Hadži, *J. Raman Spectrosc.* **2009**, *40*, 11605–11614. https://doi.org/10.1002/jrs.2308

[26] M. J. Frisch, G. W. Trucks, H. B. Schlegel, G. E. Scuseria, M. A. Robb, J.R. Cheeseman, J. A. Montgomery Jr., T. Vreven, K. N. Kudin, J. C. Burant, J. M. Millam, S. S.Iyengar, J. Tomasi, V. Barone, B. Mennucci, M. Cossi, G. Scalmani, N. Rega, G. A. Petersson, H. Nakatsuji, M. Hada, M. Ehara, K. Toyota, R. Fukuda, J. Hasegawa, M. Ishida, T. Nakajima, Y. Honda, O. Kitao, H. Nakai, M. Klene, X. Li, J. E. Knox, H. P. Hratchian, J. B. Cross, V. Bakken, C. Adamo, J. Jaramillo, R. Gomperts, R. E. Stratmann, O. Yazyev, A. J. Austin, R. Cammi, C. Pomelli, J. W. Ochterski, P. Y. Ayala, K. Morokuma, G. A. Voth, P. Salvador, J. J. Dannenberg, V. G. Zakrzewski, S. Dapprich, A. D. Daniels, M. C. Strain, O. Farkas, D. K. Malick, A. D. Rabuck, K. Raghavachari, J. B. Foresman, J. V. Ortiz, Q. Cui, A. G. Baboul, S. Clifford, J. Cioslowski, B. B. Stefanov, G. Liu, A. Liashenko, P. Piskorz, I. Komaromi, R. L. Martin, D. J. Fox, T. Keith, M. A. Al-Laham, C. Y. Peng, A. Nanayakkara, M. Challacombe, P. M. W. Gill, B. Johnson, W. Chen, M. W. Wong, C. Gonzalez, J. A. Pople, *Gaussian03*, *Revision C.02,* Gaussian, Inc., Wallingford, CT, **2004**.

[27] MOLVIB, Program developed by K. Kuczera and J. Wiorkiewicz-Kuczera at Harvard University.

[28] G. Keresztury, G. Jalsovszky, *J. Mol. Struct.* **1971,** *10*, 304–305. https://doi.org/10.1016/0022-2860(71)87090-4

[29] H. Rostkowski, L. Lapinski, M. Nowak, *Vib. Spectrosc.* **2009,** *49*, 43–51. https://doi.org/10.1016/j.vibspec.2008.04.012

[30] E. H. Ellestad, P. Klaboe, G. Hagen *Spectrochimica Acta A* **1971**, *27*, 1025–1048. https://doi.org/10.1016/0584-8539(71)80186-1

[31] C. W. Lehmann, P. Luger *Z. Kristallogr.* **1991**, *195*, 49–63. https://doi.org/10.1524/zkri.1991.195.1-2.49